

PCCP

Accepted Manuscript



This is an *Accepted Manuscript*, which has been through the Royal Society of Chemistry peer review process and has been accepted for publication.

Accepted Manuscripts are published online shortly after acceptance, before technical editing, formatting and proof reading. Using this free service, authors can make their results available to the community, in citable form, before we publish the edited article. We will replace this *Accepted Manuscript* with the edited and formatted *Advance Article* as soon as it is available.

You can find more information about *Accepted Manuscripts* in the [Information for Authors](#).

Please note that technical editing may introduce minor changes to the text and/or graphics, which may alter content. The journal's standard [Terms & Conditions](#) and the [Ethical guidelines](#) still apply. In no event shall the Royal Society of Chemistry be held responsible for any errors or omissions in this *Accepted Manuscript* or any consequences arising from the use of any information it contains.

The puzzling first-order phase transition in water-glycerol mixture

Ivan Popov¹, Anna Greenbaum (Gutina)¹, Alexei P. Sokolov^{2,3} and Yuri Feldman^{1†}

¹*The Hebrew University of Jerusalem, Department of Applied Physics, Edmond J. Safra Campus, Givat Ram, Jerusalem 91904, Israel*

²*Department of Chemistry and Joint Institute for Neutron Sciences, University of Tennessee, Knoxville, TN 37996, USA*

³*Chemical Sciences Division, Oak Ridge National Laboratory, Oak Ridge, TN 37831, USA*

Abstract

Over the last decade, discussions of a possible Liquid-Liquid Transition (LLT) has strongly intensified. The LLT proposed by several authors focused mostly on explaining the anomalous properties of water in a deeply supercooled state. However, there are no direct experimental observations yet of LLT in bulk water in the so-called ‘no man’s land’, where water exists only in the crystalline states. Recently novel experimental strategy to detect LLT in water has been employed with using water/glycerol (W/G) mixtures, because glycerol can cause a strong frustration against water crystallization. As result, the observed first-order phase transition at concentration of glycerol around $c_g \approx 20\text{mol}\%$ was ascribed to the LLT. Here we show unambiguously that the first order phase transition in W/G mixtures is caused by the ice formation. We provide additional dielectric measurements, applying specific annealing temperature protocols in order to reinforce this conclusion. We also provide an explanation, why such phase transition occurs only in the narrow glycerol concentration range. These results clearly demonstrate a danger of analysis of phase-separating liquids to gain better insight into water dynamics. These liquids have complex phase behavior that is affected by temperature, phase stability and segregation, viscosity and nucleation, and finally by crystallization, that might lead to significant misinterpretations.

Introduction

Over the past few years, many papers devoted to Liquid-Liquid Transition (LLT) have been published [1-5]. The LLT is defined as a first order phase transition between two states of the same liquid (liquid I and liquid II), which can differ by their density, refractive index, structure, glass transition temperature T_g , fragility, miscibility with other liquids [6], *etc.*. The LLT for pure water in these models [1-5] was predicted to occur in a

† Corresponding author: yurif@mail.huji.ac.il

deeply supercooled state [7-10]. This prediction was also supported by computer simulations [9, 11]. However, there are no direct experimental observations yet of LLT in bulk water, because LLT should occur in the so-called ‘no man’s land’. This is the region where bulk water exists only in crystalline states: it is below a homogeneous nucleation temperature T_H (~ 235 K at ambient pressure) and above the crystallization point of ultra-viscous water heated from low temperature [8]. Therefore, the prediction of LLT in bulk water remains as a hypothesis confirmed only by simulations using particular models. At the same time there are few approaches that are questioned the existence of the LLT transition in water (see for example [12, 13]), and suggested some alternative explanations for its unusual dynamics [14]. An intense discussion between supporters of LLT in water and its opponents was published in [15].

Recently new experimental efforts to access the ‘no man’s land’ and to identify LLT in water have been proposed. One of them is mixing the target liquid with another liquid that can prevent crystallization and reveal a hidden LLT. The easiest proposed scenario was to use the water/glycerol (W/G) mixtures, because glycerol can cause a strong frustration against water crystallization [16]. Sophisticated experiments with W/G mixtures at specific concentration around $c_g \approx 20\text{mol}\%$ indeed revealed a first-order phase transition in W/G mixtures that has been ascribed as genuine LLT of water component [16]. On the other hand, earlier detailed experimental studies of W/G glycerol mixtures in a wide range of glycerol concentrations [17-22] demonstrated that such first-order phase transition experimentally observed only in the narrow range of the glycerol concentration from $c_g \approx 15\text{mol}\%$ to $c_g \approx 28\text{mol}\%$, and it was assigned to ice formation from excess water, which is phase separated from glycerol/water mixture at lower temperatures.

To resolve this controversy we present here a comprehensive analysis of the available experimental results (including our previous results [17-22] and results presented in [16]). Our detailed analysis unambiguously suggests that the first order phase transition in W/G mixtures is caused by the ice formation. To support this conclusion, we provide additional experimental measurements with specific temperature protocols. Moreover, we also provide an explanation, why such phase transition occurs only in this specific glycerol concentration range.

In the next section, we remind the general scenario of ice formation in W/G mixtures [17-22]. Then we present the experimental measurements performed by the different techniques (BDS, DSC, X-ray scattering) to support the proposed scenario. Next, we provide detailed explanation of the observed first-order phase transition in the framework of the ice formation scenario in W/G mixtures, and define the conditions at which this phase transition may take place.

The ice formation scenario in W/G mixtures

A qualitative model of water states in W/G mixtures was presented in [17-22]. It was found that at high concentrations of glycerol all water molecules are interacting with glycerol molecules via H-bonds, creating partially coupled W/G network. Indeed, each glycerol molecule can form up to $n_g=6$ H-bonds by three OH groups [23]. However, with increase of water content, there is a critical concentration at which all the glycerol H-bonds are already occupied by water molecules. This state of the W/G mixture we will define as *the saturated W/G matrix*.

Consequently, there are excess water molecules even at slightly higher water content. They are weakly coupled with the glycerol matrix. At ambient conditions, the weakly coupled water molecules are homogeneously distributed through the whole W/G solution due to usual entropy of mixtures. We called this state of W/G mixture as *the water rich W/G matrix*. However, at low temperatures decrease of the entropic contribution to the free energy of the mixture leads to phase separation of the excess water molecules. Then these excess water domains transform into ice. Therefore, if this mixture is quenched fast, a metastable state of the excess water in solution can be achieved. In this case, the excess water diffuses from the water rich W/G matrix, forms nucleus and crystallizes into the ice via the first order phase transition. In turn, the remaining W/G matrix becomes drier and transforms into the stable saturated W/G matrix. As a result, we have the stable phase-separated state, which include both ice and saturated W/G matrix. Furthermore, a thin layer of *interfacial ice-like water* appears between the ice crystals and saturated W/G matrix. The transition temperature strongly depends on the experimental conditions: concentration of glycerol, heating rate, quenching, etc.

At low glycerol concentrations of W/G mixtures (*the over-saturated W/G matrix*), the clusters of excess water (i.e. water pools) prevail over the separately distributed water molecules in the mixture. Therefore, the ice particles are formed rapidly in these water clusters already during quenching. Consequently, after the quench the stable phase-separated states with ice crystals exist, and no any additional first order phase transition is observed on heating.

To verify unambiguously this scenario in W/G mixture, we will analyze the numerous experimental facts observed by different methods.

Experimental observations and consequences

Here we will consider the results obtained by three experimental methods: Broadband Dielectric Spectroscopy (BDS), Differential Scanning Calorimetry (DSC) and X-ray scattering (latter are from [16]).

For convenience, we'll split the whole studied concentration interval of W/G mixtures into three intervals where the experimental results are different: the first one is from $c_g=100$ mol% to $c_g\approx 28$ mol%, the second interval is from $c_g\approx 28$ mol% to $c_g\approx 15$ mol% and finally the third one is from $c_g\approx 15$ mol% to $c_g=0$ mol%. We marked these intervals in the state c - T diagram of the water/glycerol mixture [24] (Fig.1). It is worth noting, that the boundary between first and second range coincides with the eutectic point. The red region in the Fig. 1 marks the concentration range, where the LLT was claimed to be observed in [16].

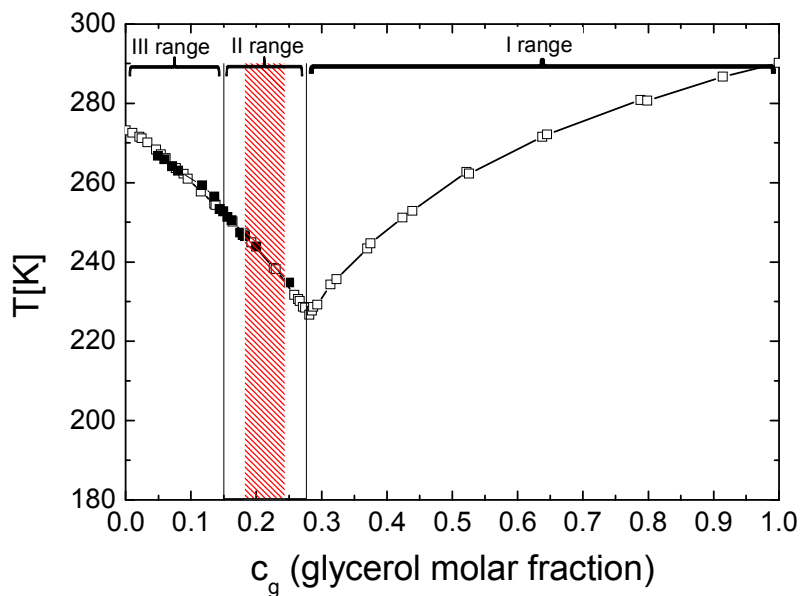
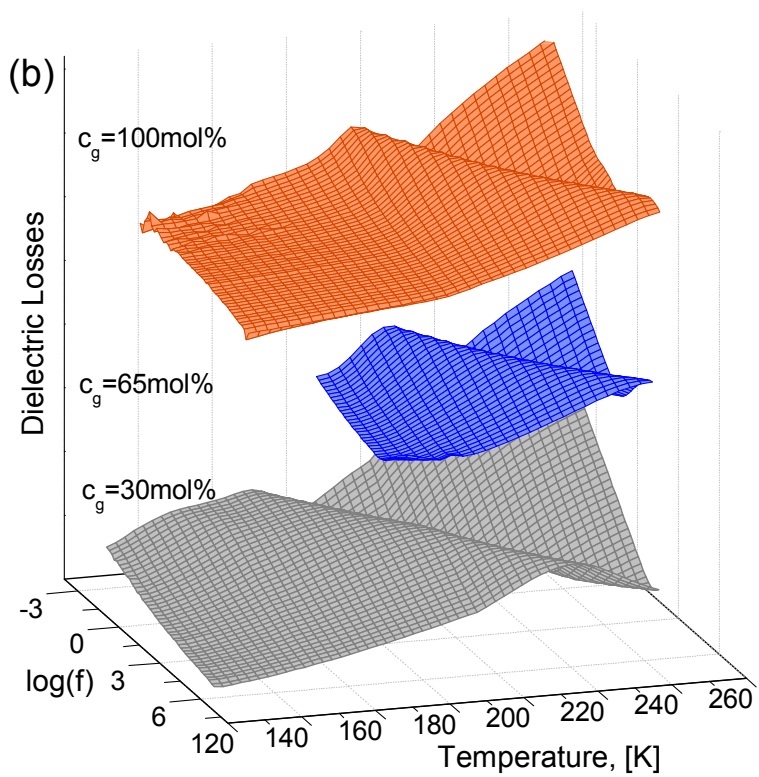
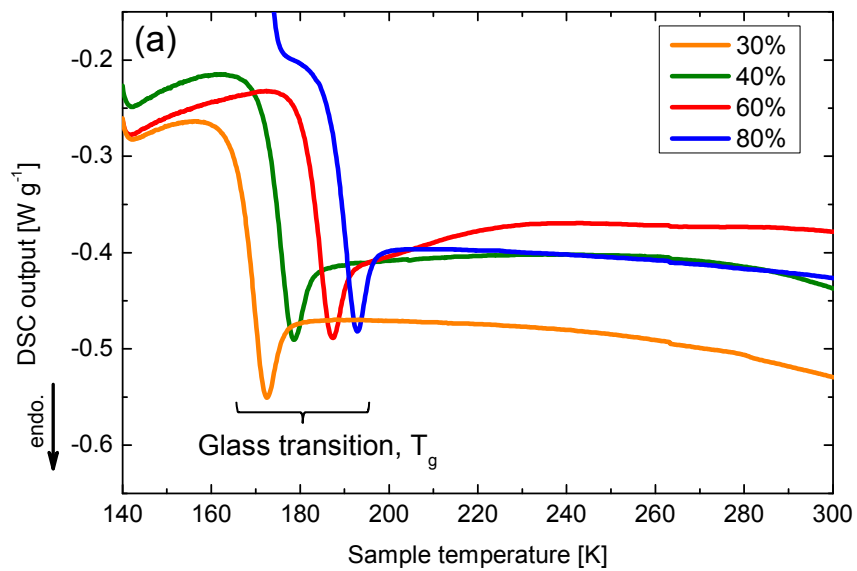


Figure 1. State diagram of the W/G mixture. Schematically division of glycerol concentrations into three ranges in dependence on water behavior in W/G mixtures. Open squares define the melting point of the water/glycerol mixture found in [24]. Black full squares were found in [16]. By red area we denote the concentration range, where LLT was observed in the measurements performed in [16].

First range: from $c_g=100\text{mol}\%$ to $c_g\approx 28\text{mol}\%$.

It is known that the glycerol is a very hydrophilic liquid. It has a great tendency to supercool, and it was found that seeding was required to obtain the true freezing points of W/G mixtures at high concentration of glycerol [24]. In our DSC measurements (Fig. 2a) we didn't use seeding, therefore no crystallization or melting was detected at glycerol concentration higher than $c_g\approx 28\text{ mol}\%$. It means that water molecules are well miscible with glycerol at these concentrations, creating a joint H-bonded network of water and glycerol and this system remains stable in a supercooled state. The DSC for glycerol concentrated mixtures shows only the glass transition in the temperature interval from 170K-195K, where T_g increases with the glycerol concentration (Fig. 2a).



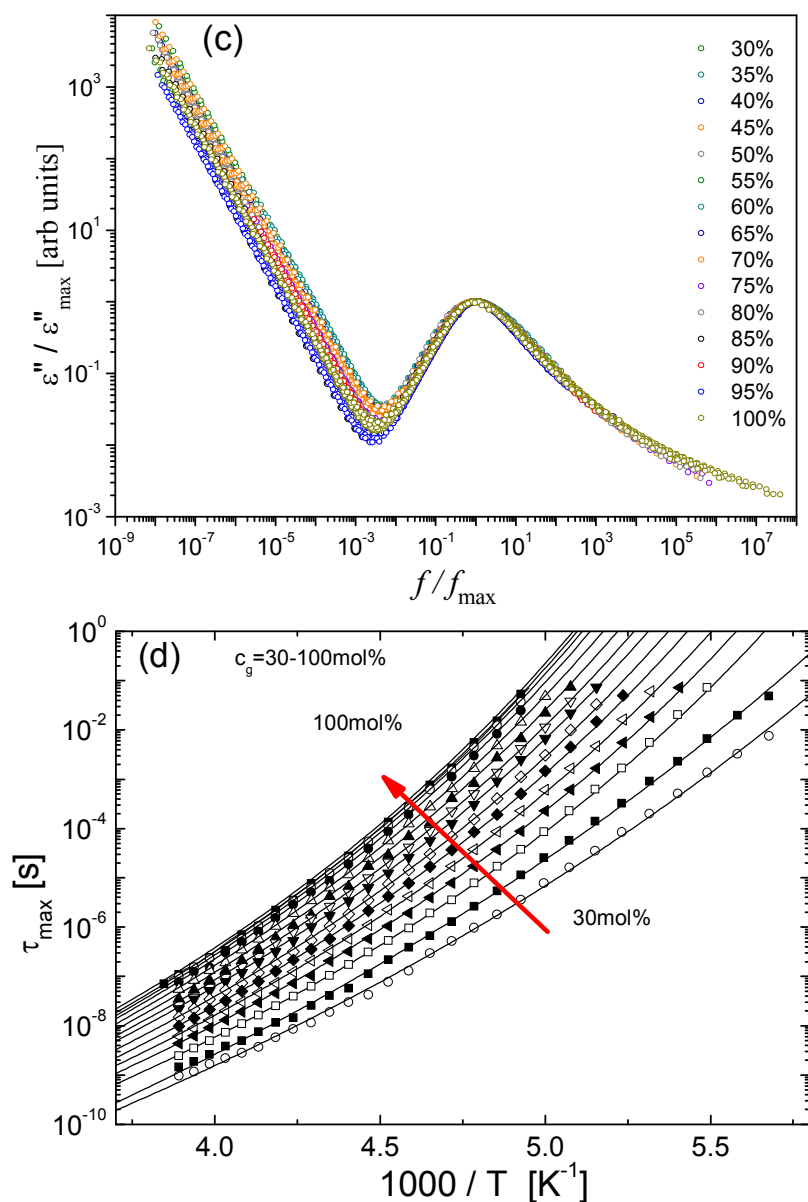


Figure 2. DCS and BDS measurements of high concentrated W/G mixtures. a) DSC data for W/G mixtures at high glycerol concentration **b)** The typical experimental data of imaginary part of complex dielectric permittivity of W/G mixtures for $c_g=100, 65, 30$ mol% are presented. **c)** Master plot of imaginary part of complex dielectric permittivity for $c_g=100-30$ mol%. **d)** The temperature dependences of the main relaxation time for the concentration glycerol range $c_g=100-30$ mol% with the step 5mol%.

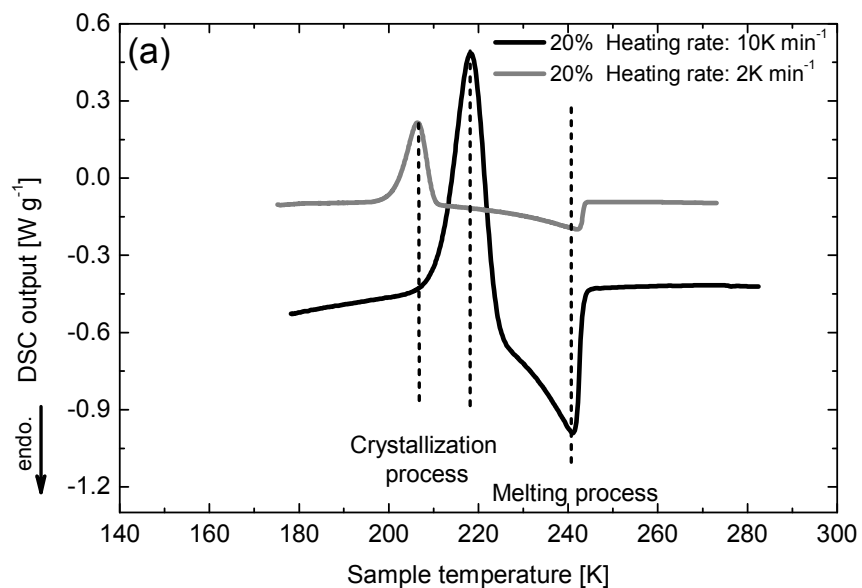
Similar results were revealed by BDS measurements, where a single relaxation process is observed at all concentrations down to 30 mol% [20] (Fig. 2b). Note that in

that case we did not use any seeding. Using a master plot presentation of the dielectric relaxation spectra, it has been demonstrated that the main relaxation process, the high frequency excess wing and the dc-conductivity exhibit the same temperature dependence [20] (Fig. 2c). The relaxation time behavior follows the Vogel-Fulcher-Tammann (VFT) law, typical for the glass formers (Fig. 2d). The glass transition temperature, T_g , evaluated from BDS data drops with decrease of the glycerol concentration, in agreement with the DCS measurements [20] (Fig. 2a). These results suggest that there is no phase separation in these mixtures even at very low temperatures, and the main relaxation peak corresponds to the structural relaxation in homogeneous W/G mixtures [25].

Second range: from $c_g \approx 28 \text{ mol\%}$ to $c_g \approx 15 \text{ mol\%}$.

The DSC data of this region is significantly different in comparison with the first one. The exothermic peak (Fig. 3a) corresponding to the first-order phase transition is observed only in this region. Here we present the data for $c_g \approx 20 \text{ mol\%}$. The existence of the first-order phase transition for $c_g \approx 16.5$ and 17.8 , mol% was claimed in [16]. In our DSC data, the peak position and its shape depend strongly on the heating rate. At the faster heating rate, the peak shifts to higher T and partly overlaps the temperature interval of the broad melting peak. However, at slow rates, no overlap is observed, and we can estimate the enthalpy of the first-order phase transition for both exothermic and endothermic processes by integration of the heat capacity relative to the baseline. For $c_g \approx 20$ mol% in both cases, we obtained approximately the same value. The endothermic process is caused only by ice melting (see the state diagram, Fig. 1). This is the reason that the same value of ΔH suggests that the exothermic peak of the first-order phase transition corresponds to the ice crystallization process only. Furthermore, the ice

formation is observed by the X-ray scattering experiments. The growth of two peaks related to ice [26] is clearly observed with time evolution measurements (Figs. 3c,d in [16]). The measurements in [16] were performed at the very low annealing temperature and we believe that this is the reason that the ice formation takes very long time. At lower annealing temperatures, the crystallization is slower due to the higher viscosity, and during given time interval less amount of ice can be formed than at high temperatures. This point is supported by the X-ray data presented in Figs. S3a and S3b in [16]. The data provide additional evidence that the first-order phase transition observed as an exothermic peak in the DSC measurements (Fig. 3a) should involve ice formation. At the same time in [16] this transition was ascribed to LLT.



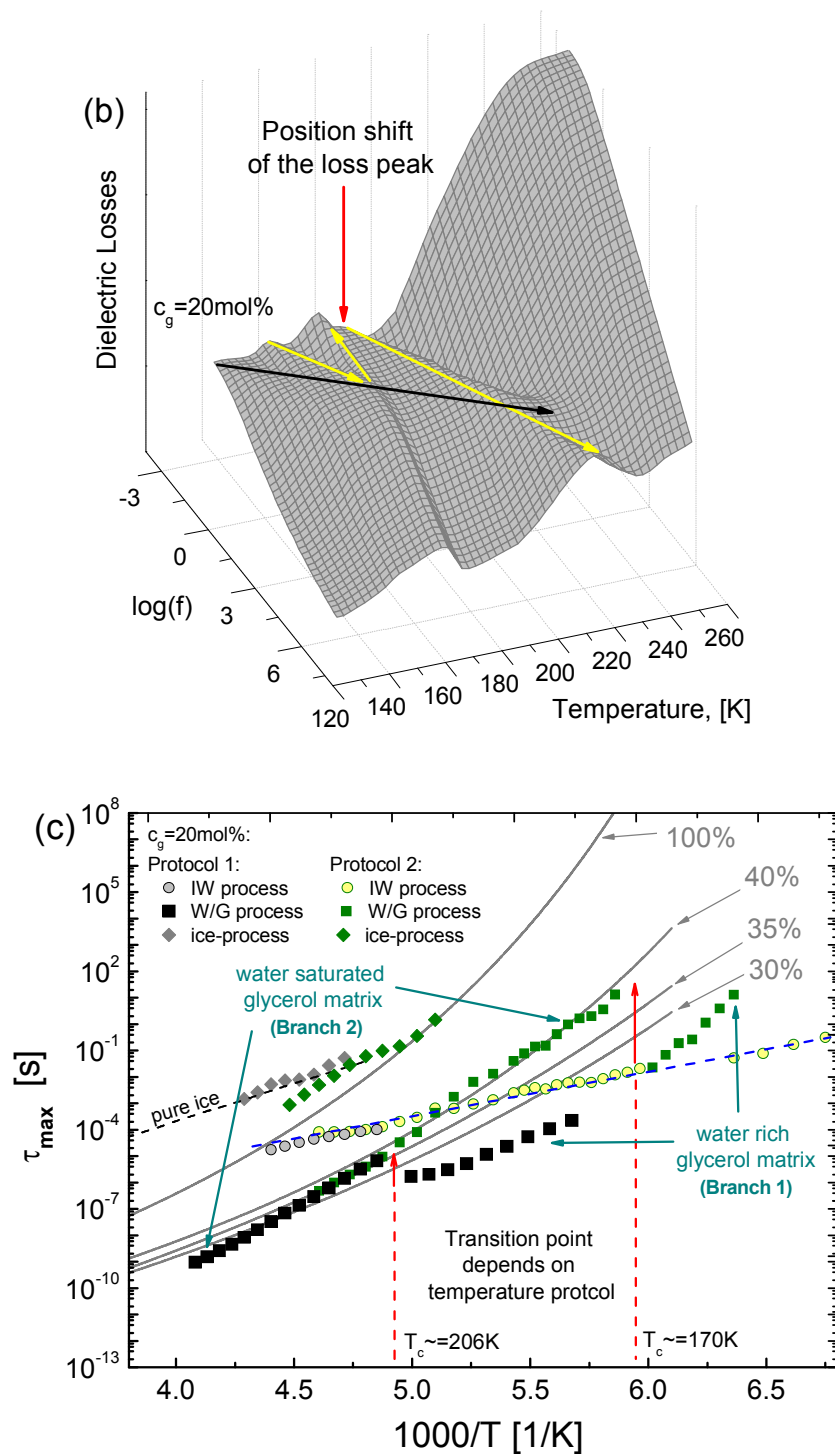


Figure 3. The DCS and BDS data for W/G mixtures at $c_g=20\text{mol}\%$. **a)** DCS data for $c_g=20\text{mol}\%$. Besides of melting process and glass transition, we can observe the clear exothermic peak (here we concentrated only on exothermic peak, and didn't measure in range of temperature with glass transition. The existence of glass transition can be found in [16]). **b)** The 3D graph of temperature and frequency dependences of imaginary part of complex dielectric permittivity for

$c_g=20\text{mol}\%$. In this 3D plot, we clearly see two peaks (third peak reveals at low frequency range and not clearly seen in 3D graph, only in a cross-sections [20]). The moving of one of them with increasing temperature we labeled by black line, the trajectory of the peak of another one we marked by yellow line. The sharp shift of the position of the loss peak is pointed out by red arrow; **c)** The temperature dependences of the relaxation time of losses peaks in both temperature protocols. Non colored points: black squares, grey diamonds, grey circles correspond to the observed loss peaks in Protocol 1 [17, 18, 20]. Colored points: green squares, green diamonds, yellow circles obtained via Protocol 2.

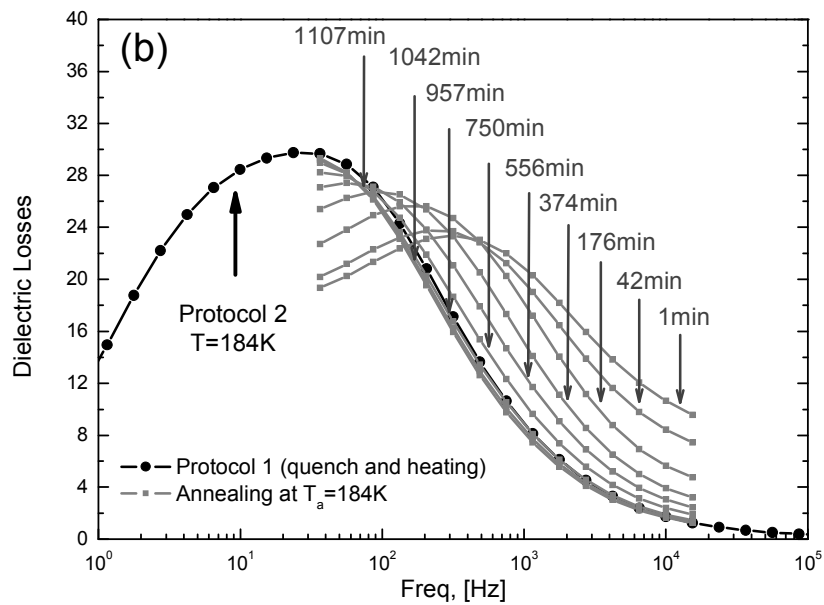
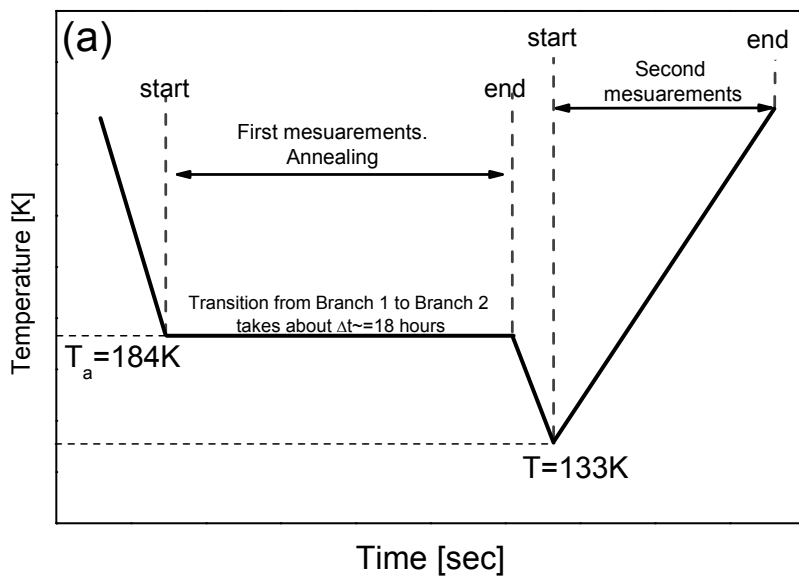
In the framework of ice formation scenario, it is easy to explain the results of BDS measurements in this particular glycerol concentration region that were performed with the following temperature protocols [17, 18, 20] (sec. Materials and Methods):

Protocol 1: BDS measurements were provided in the frequency range from 1Hz to 250MHz at temperatures from 173 to 273 K at intervals of 3 K.

Protocol 2: We repeated previous measurements, but decreased the lowest temperature values, and broaden the frequency range. BDS measurements were performed in the frequency range from 0.01Hz to 250MHz at temperatures from 133 to 273 K at intervals of 3 K and the step of 1K in the vicinity of 170K.

In both protocols, the sample was quenched to the lowest temperature and then dielectric measurements were started. Here we present the results for $c_g=20\text{ mol}\%$. The similar results for $c_g=17.8\text{ mol}\%$ were published in [16]. The 3D plot of the dielectric losses versus temperature and frequency obtained via the Protocol 2 is presented in figure 3b (note that for the Protocol 1 the 3D plot looks similar). Both protocols lead to three loss peaks observation in the dielectric spectra. The temperature dependences of their relaxation time τ are presented in figure 3c. One of the processes demonstrates the sharp shift in its relaxation time τ at some transition temperature T_c (depicted by the red arrow in the figure 3b). Note that the value of this T_c differs for the two Protocols used.

The processes marked by diamonds in both Protocols are due to the presence of the ice since the relaxation time τ and its activation energy are similar to the well-known values for bulk ice (depicted by dashed black line) reported in [27, 28]. The processes marked by circles in both Protocols are due to the interfacial ice-like water (IW). It is worth noting that the activation energy of ~ 33 kJ/mol of the relaxation process resulting from IW is similar to the reported values of the activation energy for hydrated water in different systems [29, 30]. The processes marked by squares correspond to α -relaxation of W/G matrixes in its different state. Below T_c the data in both Protocols belongs to the same temperature behavior (Branch 1), which lies under the curve corresponding to $c_g=30$ mol%. It means that Branch 1 corresponds to the water rich W/G matrix. After transition above T_c , the relaxation times belongs to another curve (Branch 2), which now coincides with the data for the $c_g=30-40$ mol% samples. It means that W/G matrix turned to be more “dry” at T above T_c . In another words, as we defined earlier, it forms the stable saturated W/G matrix. The excess water expelled from the W/G matrix transforms into the ice and appears as a typical ice relaxation process in the dielectric spectra (marked by diamonds, Fig. 3c). Note that the saturated W/G matrix does not crystallize and stay in the super cooled state. The critical temperature T_c depends strongly on the temperature protocol ($T_c \approx 206$ K for the Protocol 1 and $T_c \approx 170$ K for the Protocol 2) and shows that water in the rich W/G matrix is in the metastable state. This transition moves to the high temperatures with the heating rate increase. The Protocol 2 required the measurements at much lower frequency range that automatically means slower heating in comparison with the initial Protocol 1. It correlates with the DSC data (Fig 3a).



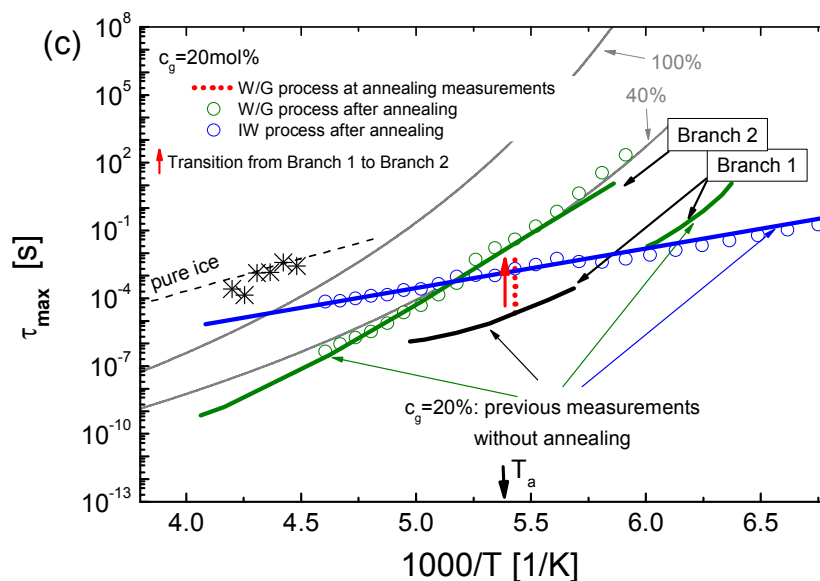


Figure 4. BDS measurements W/G mixtures at $c_g=20\%$ mol. Special protocol. a) The details of the special annealing temperature protocol: after quench down to $T_a=184\text{K}$, we made annealing of the sample until the transition from Branch 1 to Branch 2 is occurred. It takes about 18 hours. After the transition, the sample was cooled down to $T=133\text{K}$. At this point, the BDS measurements start again with the heating up to the final temperature 273K . **b)** The shift of the peak position under annealing procedure at $T_a=184\text{K}$ (grey lines). The black line denotes the dielectric measurement, which was obtained according to Protocol 2 at 184K (see the text). **c)** The temperature dependences of the relaxation times obtained from BDS measurements performed via annealing temperature protocol. The results of annealing measurement are shown by red circles. The shift direction of the loss peak position associated with W/G matrix is depicted by red arrow. Open green and blue circles, and black snowflakes correspond to the results obtained from the second measurement of the current protocol via heating. The data obtained previously without annealing from Protocols 1 and 2 are depicted by solid lines: green, black and blue lines correspond to the data from figure 3c, the grey lines correspond to the data from figure 2d.

The metastable water in the water rich W/G matrix can initiate the transition from Branch 1 to Branch 2 at any temperature, even at annealing procedure without heating. To verify this assumption we quenched the sample down to $T_a=184\text{K}$ and made an annealing at this temperature, performing simultaneously the BDS measurement (see Materials and Methods and Fig. 4a). We specifically selected this temperature point as the one between the T_c 's obtained in previous Protocols. The figure 4b shows a clear shift of the loss peak that corresponds to transition from the water rich (Branch 1) to the

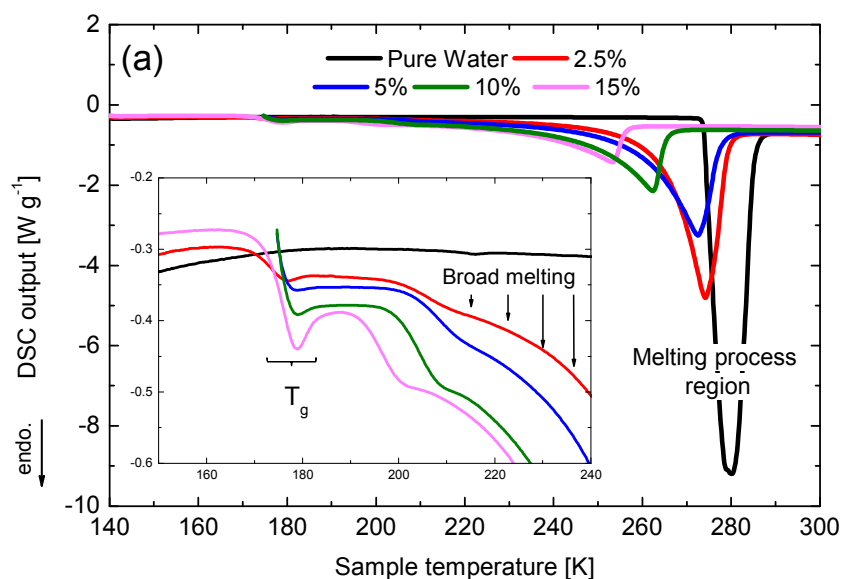
saturated W/G matrix (Branch 2) at the annealing temperature T_a . In the figure 4c this transition is marked by red arrow. This transition took about 18 hours, which is much longer in comparison with the previous experiments (Fig 3c), where the duration of the transitions was about several minutes. After the transition at T_a we quenched the sample down to $T=133\text{K}$ and started the BDS measurements (0.01Hz to 250MHz) on the heating mode from 133 to 273K with the step 3K. As a result, only the relaxations of the saturated W/G matrix, ice and interfacial water are observed without any reversible transition of the water (Fig 4c). Note that Maxwell-Wagner surface polarization [31] doesn't contribute significantly in the considered frequency range. Based on the estimation values of the conductivity and permittivity of the W/G mixture performed in [18], we may conclude, that Maxwell-Wagner relaxation occurs in the lower frequency range regarding of the slowest ice process.

Third range: from $c_g \approx 15\text{mol}\%$ to $c_g \approx 0\text{mol}\%$.

In this range of glycerol concentrations, there are enough excess water molecules to create ice crystals in the bulk W/G mixture during its cooling below the water crystallization point. The DSC data in this range are clearly indicating the melting process of ice (Fig. 5a), which correlate with the data in the state diagram (Fig.1). Note that in this case the exothermic peak is not observed because water has crystallized already during the cooling.

The BDS data (Fig. 5b) always show three loss peaks without any sharp transitions at glycerol concentration less than 15 mol% (as it was observed in Fig 3b,c and 4b). The relaxation times of the corresponded loss peaks are independent of glycerol

content and coincides with each other (See colored ovals in figure 5c). The relaxation times marked by green oval coincide with Branch 2, which corresponds to the saturated W/G matrix relaxation process. The sets highlighted by the blue and pink ovals correspond to IW and ice relaxation processes, respectively. The results support the scenario suggested above, that there is a phase separation, forming saturated W/G phase, and the excess water transforms into the ice during the cooling. Therefore, even in the starting measurements at the lowest temperature we already have the ‘dry’ saturated W/G matrix, ice particles and IW layer between them.



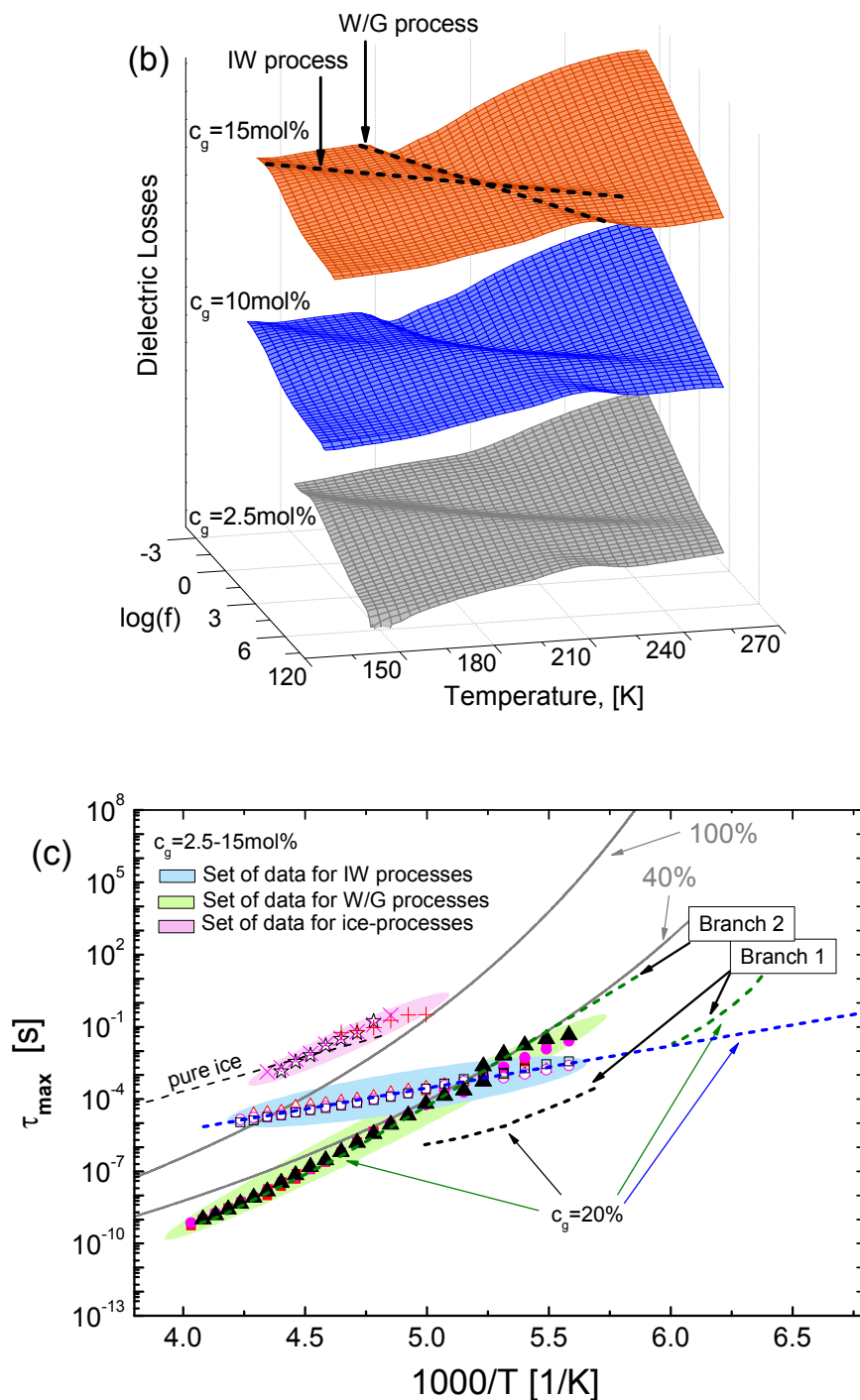


Figure 5. The DSC and BDS data for W/G mixtures at low concentration of glycerol. a) In DSC data for low concentration of glycerol from 0 mol% up to 15 mol% we have one glass transition at low temperature and broad melting region. As one would expect the melting point decreases with increasing of the concentration. **b)** The typical experimental data of imaginary part of complex dielectric permittivity of W/G mixtures for $c_g = 15, 10, 2.5 \text{ mol\%}$ are presented. All 3D graphs looks similar. In all of them, we clearly see two crossed processes, which correspond to

IW process and W/G matrix process. Third process, which correspond to the ice is not clearly observed in 3D graph and can be revealed on temperature cross-sections [20]. **c)** In the figure the temperature dependences of relaxation time correspond to three observed processes are presented. The behaviors of the corresponding losses peaks for different glycerol concentration are the same. The set of data for different glycerol concentration related to ice processes is outlined by pink oval; the set of data correspond to interfacial water (IW) processes is outlined by blue oval; the set of data correspond to saturated W/G matrix process is outlined by green oval. Also we represent the several data from previous experiments (from Fig 2d and 3c) by different lines.

Critical concentration range. The behavior of the metastable excess water in W/G mixtures

Based on the properties of glycerol and water molecules one can estimate the range of concentrations where the formation of the metastable state of excess water in W/G mixture is available. Consequently, only in this concentration region, we can observe the spontaneous water crystallization via first-order phase transition. Hereinafter we call this range as a critical one. Relying on the experimental results, we found that this interval is around $c_g \approx 28-15\text{mol}\%$.

As we mentioned above, every glycerol molecule can form up to $n_g=6$ H-bonds by three OH^- groups [23]. Without water every glycerol molecule interacts with its neighbors by these H-bonds. Thus at the concentration of glycerol $c_g = 100\text{mol}\%$ we have the direct glycerol-glycerol ($\text{G}\cdots\text{G}$) interaction only. According to our scenario, increasing of the water content forms the miscible W/G system, with the water molecules evenly distributed inside of glycerol matrix without creating any water “pools”. Thus, water molecules are incorporated into the glycerol network, destroying the direct $\text{G}\cdots\text{G}$ interaction and forming the new links, such as $\text{G}\cdots\text{W}\cdots\text{G}$ (glycerol-water-glycerol). Consequently, with water content grow, the fraction N_{GG} of $\text{G}\cdots\text{G}$ interactions decreases, while the number of $N_{G\text{WG}}$ of $\text{G}\cdots\text{W}\cdots\text{G}$ increases. At some *minimum* value of glycerol

concentration the fraction of $N_{GG} \rightarrow 0$. Since every glycerol molecule has $n_g=6$ H-bonds, then there are $n_g/2$ water molecules per one glycerol molecule. It corresponds to the concentration value:

$$c_g^{up} \approx 100\% \times \frac{1}{1+n_g/2} \approx 25\text{mol}\%, \quad (1)$$

which approximately coincide with upper boundary of the critical concentration range. In the glycerol concentration between 100mol% and c_g^{up} the W/G mixture represents itself as a stable 3D H-bond network. Therefore, different experimental technique provides similar structural and dynamic properties of these mixtures with a variation of T_g (See Figs 2a and 2d).

The further water content increase leads to an excess water and the new scenario of water glycerol interactions. In that case, the system can be heterogeneous with coexisting of separate water pools. At room temperature at some water concentration every glycerol molecules is surrounded by its own salvation shell, i.e. there are $n_g = 6$ water molecules per one glycerol molecule

$$c_g^{down} \approx 100\% \times \frac{1}{1+n_g} \approx 14.2\text{mol}\%, \quad (2)$$

which approximately coincide with the lower boundary of the critical concentration range. If concentration of glycerol is less than c_g^{down} , the water clusters (pools) always exist in W/G mixture, because all of H-bonds of glycerol are occupied. It is worth noting, that boundary of the critical range depends on cooling rate and can shift.

The behavior of W/G mixtures below c_g^{down}

As mentioned above in the range of glycerol from c_g^{down} to 0 mol% water clusters (pools) always exist. At these concentrations, there is enough water to create the bulk ice at low temperatures during quenching process. Therefore, we always observe the ice contribution in the different experimental observations, discussed above. The W/G matrix at this concentration contains only water molecules, which are H-bonded to glycerol molecules. All excess water extracts from this matrix and crystallized. We called this state as a saturated W/G matrix. In the bulk, below 0°C, at normal pressure water is crystallizing into the regular ice Ih. However, the presence of W/G matrix affects the structure of ice near its boundary by geometrical factor (by roughness of an interface boundary) or by binding factor (different H-binding in ice and glycerol). In any case the dynamic in this water layer should be different in comparison to dynamic in W/G matrix or bulk ice. We defined this layer as an interfacial ice-like water (IW). Schematically it is presented in figure 6a. Thus a three component system is stable (saturated W/G matrix, ice particles and interfacial ice-like water). Therefore, BDS spectra in this glycerol concentration range (Fig. 5b, c) exhibit only three corresponding processes without any phase transitions.

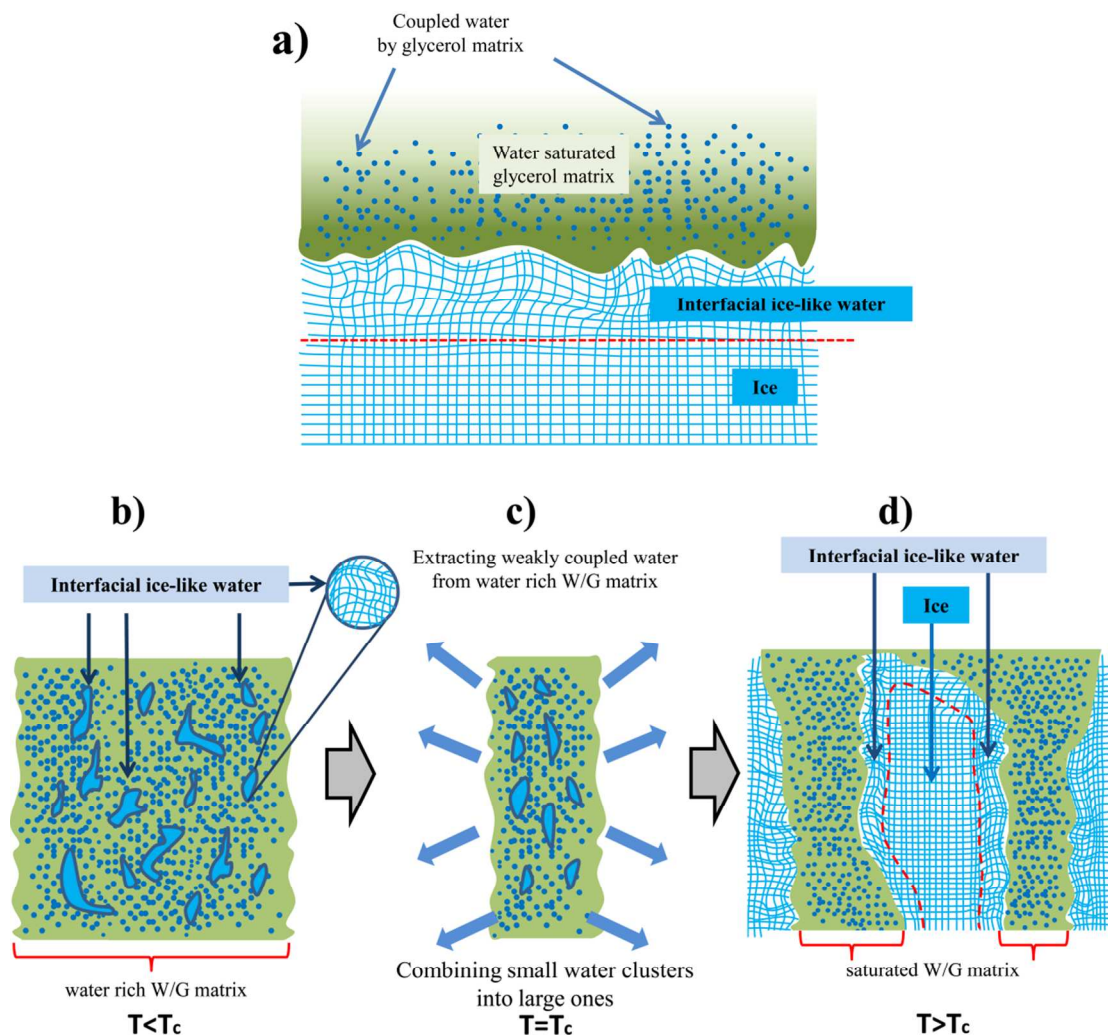


Figure 6. a) Schematic representation of W/G mixture at low temperature and at low concentration of glycerol. b)-d) Schematic presentation of ice formation in W/G mixtures in the critical concentration range.

The behavior of W/G mixtures in critical range from c_g^{up} to c_g^{down}

In the critical range from c_g^{up} to c_g^{down} the excess water clusters don't create large water pools in saturated W/G matrix. We assume that these small water clusters at room temperature are evenly distributed inside the W/G network. At low temperatures, after the quench, the phase separation on saturated W/G domains and excess water clusters starts.

This process might be slow due to very high viscosity and initial water clusters are smaller than the critical ice nucleus. Therefore, these water clusters behave as an interfacial water (see Fig. 6b). However, their uniform distribution in W/G mixture affects the behavior of W/G matrix. This state of W/G matrix we defined above as a water rich W/G matrix. As a result, below T_c we observed two dielectric loss peaks related to the ice-like interfacial water and water rich W/G matrix (Branch 1 in Figs. 3c). Schematically we can present this situation as: *Initial state ($T < T_c$) = water rich W/G matrix + interfacial ice-like water;*

With heating or annealing, as it follows from BDS, DSC, X-ray measurements, the ice particles appear and start to grow. Furthermore, from BDS, above T_c the process related to W/G matrix behaves itself like saturated W/G mixture at high concentration of glycerol (see Fig. 3c). It means that excess water phase separates from the water rich W/G matrix (See Fig. 6c). It leads to growth of the ice particles and as a consequence the appearance of a regular (ordered) ice structure. In turn the W/G matrix becomes drier. The interfacial ice-like water layer appears between W/G matrix and ice content (see Fig. 6d). As a result, above T_c we observed the three-component system: *Final state ($T > T_c$) = water saturated W/G matrix + interfacial ice-like water + ice;* At lower temperatures the dynamic of phase separation is slower due to higher viscosity [16].

Conclusions

In summary we conclude that the spontaneous ice formation on heating is possible only in the narrow glycerol concentration range (second range in the state diagram of the W/G mixture (See Fig.1)). Exactly in this interval of glycerol concentration the observed first-order phase transition was attributed to LLT in [16]. The LLT in W/G mixture

wasn't detected outside of this range in [16]. It indicates that the observed phase transition is the genuine ice formation. Our results and analysis show very clear a danger of analysis of unstable mixtures, where the phase transition can be a consequence of the phase separation and following crystallization. The attempt to use these kinds of mixtures outside of their miscibility region to study bulk water properties might lead to significant misinterpretations and misleading conclusions.

Materials and Methods

Water/glycerol (W/G) mixtures with glycerol content from 0 mol% to 100 mol% were prepared from anhydrous glycerol (product number 49767, Fluka, Buchs, Switzerland) and double distilled water.

Differential scanning calorimetric (DSC) measurements for W/G mixtures were performed using DSC 2920 calorimeter (TA Instruments) in wide range of molar glycerol concentration for the temperature interval from 138K to 313K. The all samples were quenched and then heated up. The heating rate for all concentrations was 10K min^{-1} . For concentration of glycerol $c_g=20$ mol% we repeated DSC measurements at different heating rate: for 10K min^{-1} and for 2K min^{-1} . The additional details of these experiments can be found in our previous work [17, 18].

Broadband Dielectric Spectroscopy (BDS) measurements of W/G mixtures at different concentrations were performed using a Novocontrol BDS-80 and RF Impedance analyzer. In all experiments (if it is not specifically mentioned) the samples was quenched to lowest temperature, then the dielectric measurements at stabilized temperature points was performed by further heating from 173K up to 273K at intervals of 3 K. The additional details of these experiments can be found in our previous works

[18, 19]. Two additional new experiments were performed to support the scenario of ice formation in W/G mixtures. First, we repeated the study of $c_g=20$ mol%, where the controversial LLT was predicted around 170K [16]. However, in that case the sample was quenched to the lower temperature 133 K. The measurements were provided up to 273 K with the step 3 K, but in the vicinity of 170K the step was 1K (In the text we called this protocol as Protocol 2).

In addition, for $c_g=20$ mol% we applied the special temperature protocol with an annealing. In this protocol the sample was quenched down to 184K, after that the annealing was started. At annealing procedure the measurements were provided in the frequency range from 36Hz to 15.3kHz. Unlike the Protocols 1 and 2 we restricted the frequency range, because we worried to not miss the transition (in the Protocols 1 and 2 it took several minutes). However, contrary to our expectations in this case the transition took around 18 hours. After transition we quench the sample down to 133K and started the BDS measurements (0.01Hz to 250MHz) on the heating mode from 133 to 273 K with the step 3 K (see Fig. 4a).

Acknowledgments

The authors are grateful to Prof H. Tanaka for initiation of this work and comprehensive discussions. The work was supported by the Valazzi-Pikovsky Fellowship (Lady Davis Fellowship). The work was partly supported by the Russian Government Program of Competitive Growth of Kazan Federal University. APS thanks NSF Chemistry program (grant CHE-1213444) for partial financial support.

References

1. K. Murata and H. Tanaka, *Nat Commun*, 2013, **4**.
2. H. Tanaka, *Faraday Discuss*, 2013, **167**, 9-76.

3. J. C. Palmer, F. Martelli, Y. Liu, R. Car, A. Z. Panagiotopoulos and P. G. Debenedetti, *Nature*, 2014, **510**, 385-388.
4. J. Russo and H. Tanaka, *Nat Commun*, 2014, **5**.
5. G. Franzese and H. E. Stanley, *J Phys-Condens Mat*, 2007, **19**.
6. R. Kurita, K. Murata and H. Tanaka, *Nat Mater*, 2008, **7**, 647-652.
7. C. A. Angell, *Annu Rev Phys Chem*, 2004, **55**, 559-583.
8. O. Mishima and H. E. Stanley, *Nature*, 1998, **396**, 329-335.
9. P. G. Debenedetti, *J Phys-Condens Mat*, 2003, **15**, R1669-R1726.
10. P. G. Debenedetti and H. E. Stanley, *Phys Today*, 2003, **56**, 40-46.
11. P. H. Poole, F. Sciortino, U. Essmann and H. E. Stanley, *Nature*, 1992, **360**, 324-328.
12. D. T. Limmer and D. Chandler, *J Chem Phys*, 2011, **135**.
13. D. T. Limmer and D. Chandler, *J Chem Phys*, 2013, **138**.
14. C. Gainaru, A. L. Agapov, V. Fuentes-Landete, K. Amann-Winkel, H. Nelson, K. W. Koster, A. I. Kolesnikov, V. N. Novikov, R. Richert, R. Bohmer, T. Loerting and A. P. Sokolov, *P Natl Acad Sci USA*, 2014, **111**, 17402-17407.
15. P. Molinero, P. Tanaka, P. Chandler, D. Limmer, P. Wynne, P. Angell, D. Soper, D. Palmer, P. Mallamace, P. Caupin, P. Evans, P. Anisimov, P. Meuwly, P. Barrat, P. Ben-Amotz, P. Wang and Wexler, *Faraday Discuss*, 2013, **167**, 109-143.
16. K. I. Murata and H. Tanaka, *Nat Mater*, 2012, **11**, 436-443.
17. Y. Hayashi, A. Puzenko and Y. Feldman, *J Phys Chem B*, 2005, **109**, 16979-16981.
18. Y. Hayashi, A. Puzenko, I. Balin, Y. E. Ryabov and Y. Feldman, *J Phys Chem B*, 2005, **109**, 9174-9177.
19. A. Puzenko, Y. Hayashi, Y. E. Ryabov, I. Balin, Y. Feldman, U. Kaatzte and R. Behrends, *J Phys Chem B*, 2005, **109**, 6031-6035.
20. Y. Hayashi, A. Puzenko and Y. Feldman, *J Non-Cryst Solids*, 2006, **352**, 4696-4703.
21. Y. Hayashi, A. Puzenko and Y. Feldman, *AIP Conference Proceedings* 2006, **832**, 99-108.
22. A. Puzenko, Y. Hayashi and Y. Feldman, *J Non-Cryst Solids*, 2007, **353**, 4518-4522.
23. J. A. Padro, L. Saiz and E. Guardia, *J Mol Struct*, 1997, **416**, 243-248.
24. L. B. Lane, *Ind Eng Chem Res*, 1925, **17**, 924.
25. S. Capaccioli, K. L. Ngai and N. Shinyashiki, *J Phys Chem B*, 2007, **111**, 8197-8209.
26. A. V. Hippel, *Ieee Transactions on Electrical Insulation*, 1988, **23**, 825-840.
27. R. Auty and R. H. Cole, *J Chem Phys*, 1952, **20**, 1309-1314.
28. S. R. Gough and D. W. Davidson, *J Chem Phys*, 1970, **52**, 5442-&.
29. N. Shinyashiki, W. Yamamoto, A. Yokoyama, T. Yoshinari, S. Yagihara, R. Kita, K. L. Ngai and S. Capaccioli, *J Phys Chem B*, 2009, **113**, 14448-14456.
30. K. L. Ngai, S. Capaccioli, S. Ancherbak and N. Shinyashiki, *Philos Mag*, 2011, **91**, 1809-1835.
31. S. Takashima, *Electrical Properties of Biopolymers and Membranes*, IOP Publishing, Philadelphia, 1989.